M. GRUBER*[#], S. PLOBERGER**, G. RESSEL*, M. WIESSNER*, M. HAUSBAUER**, S. MARSONER*, R. EBNER*

EFFECTS OF THE COMBINED HEAT AND CRYOGENIC TREATMENT ON THE STABILITY OF AUSTENITE IN A HIGH CO-NI STEEL

WPŁYW ZŁOŻONEJ OBRÓBKI CIEPLNEJ – GRZANIA I KRIOGENICZNEGO CHŁODZENIA NA STABILNOŚĆ AUSTENITU W WYSOKOSTOPOWEJ STALI CO-NI

The stability of austenite is one of the most dominant factors affecting the toughness properties of high Co-Ni steels such as Aermet 100 and AF1410. Thus, the aim of this work was to get a deeper understanding on the impact of combined heat and cryogenic treatment on the stability of retained and reverted austenite. In order to characterize the evolution of the phase fraction of austenite during tempering at different temperatures and times, X-ray diffraction analyses were carried out. The stability of austenite, which was formed during tempering, was analyzed with dilatometric investigations by studying the transformation behavior of the austenite during cooling from tempering temperature down to -100°C. Additionally, transmission electron microscopy investigations were performed to characterize the chemical composition and phase distribution of austenite and martensite before and after tempering.

Keywords: high Co-Ni steel, reverted austenite, retained austenite, high temperature X-ray diffraction, dilatometer investigations

Stabilność austenitu jest jednym z najbardziej dominujących czynników mających wpływ na ciągliwość stali Co-Ni, takiej jak Aermet 100 i AF1410. Celem pracy było głębsze zrozumienia wpływu skojarzonego nagrzewania i obróbki kriogenicznej na stabilność austenitu szczątkowego i przemienionego. Ewolucję udziału fazy austenitycznej podczas odpuszczania w różnych temperaturach i czasach przeprowadzono stosując rentgenowskie badania dyfrakcyjne. Stabilność austenitu, który powstał podczas odpuszczania, badano metodą dylatometryczną, analizując zachowanie się austenitu podczas odpuszczania w temperaturach poniżej –100°C. Zrealizowano badania metodą mikroskopii elektronowej w celu określenia składu chemicznego i rozkładu austenitu i martenzytu przed i po odpuszczaniu.

Słowa kluczowe: stal Co-Ni, austenite przemieniony, austenite szczątkowy, rentgenowska dyfraktometria wysokotemperaturowa, dylatometria

1. Introduction

High Co-Ni hardening steels are well-known for their excellent toughness properties in combination with good hardness and strength values [1-3]. Their favorable mechanical properties are mainly related to the toughening effect of austenite. In particular, in this type of steel it must be distinguished between retained and reverted austenite. Retained austenite is defined as the untransformed austenite after quenching from austenitization temperature to room temperature or even after cryogenic treatment. Conversely, reverted austenite is formed after quenching during a subsequent tempering treatment [2,4]. Generally, the toughening effect of austenite can be characterized by its stability – the resistance against transformation [5]. It is assumed that the higher the stability of austenite is, the higher is also the toughening effect of austenite. The stability of austenite is affected by its chemical composition and the size of austenite grains [6]. It is reported that austenite grains exhibit increasing resistance against transformation with decreasing size [7]. Haidemenopoulos [5] claimed that this is a result of the lower number of potential nucleation sites for phase transformation due to smaller grain sizes. In contrast to this, it is described in [8] that transformation of small austenite grains in shape memory alloys is harder because of the increasing energy barrier for transformation with decreas-

*   MATERIALS CENTER LEOBEN FORSCHUNG GMBH, ROSEGGERSTRASSE 12, LEOBEN, A-8700 AUSTRIA

**   BÖHLER EDELSTAHL GMBH & CO KG, MARIAZELLER STRASSE 25, KAPFENBERG, A-8605 AUSTRIA

[#]   corresponding Author: Marina.Gruber@mcl.at

ing grain size. Additionally, chemical stabilization of austenite can occur owing to an enrichment of austenite stabilizers, such as carbon, nickel or manganese [5,6,9,10]. In Aermet 100, which is one of the most prominent steel types of high Co-Ni hardening steels, both retained and reverted austenite are present [2]. Compared to reverted austenite the size and composition of retained austenite cannot easily be varied for toughening effects due to tempering treatment [5]. Consequently, cryogenic treatment is commonly applied to reduce the content of retained austenite and subsequent tempering treatment is employed in order to get an intended formation of reverted austenite [5]. In Aermet 100 reverted austenite is created above tempering temperatures of approximately 450°C [2,11]. Lippard [12] and Ayer, Machmeier [2] described that in Aermet 100 reverted austenite is formed predominantly at martensite lath boundaries and is enriched in nickel and depleted in cobalt.

Literature dealing with stabilization of retained austenite of steels, which are tempered above 400°C, i.e. in the temperature range where carbide precipitation occurs, is limited. In contrast to this, there are several calculations and qualitative evaluations of the stability of reverted austenite in high Ni-Co steels [5,12,13]. However, there are only a few experimental results on the stability of austenite in high Co-Ni steels at all. Consequently, the aim of this work is to present experimental results on the stability of retained and reverted austenite due to tempering and cryogenic treatment in a 0.22% C, 11% Ni, 13.5% Co, 2.9% Cr, 1.2% Mo steel.

To this end quantitative X-ray diffraction (XRD) analyses were carried out before and during tempering treatment to determine the austenite content. Transmission electron microscopy (TEM) investigations were conducted before and after tempering to analyze austenite distribution and composition. Dilatometric measurements were employed on cryogenically and on non-cryogenically treated samples to characterize the transformation behavior of austenite during cooling of specimens to room or even lower temperature after the tempering treatment. The investigations allow to draw conclusions on the effect of cryogenic treatment (CT) and different tempering treatments on the stability of austenite.

1. Experimental

The experiments were employed on a steel with a chemical composition listed in Table 1. The contents of substitutional elements were determined by X-ray fluorescence analysis and the carbon content was characterized by thermal combustion analysis.

TABLE 1

Chemical composition of the investigated steel in wt.%

	C	Ni	Co	Cr	Mo
wt.%	0.22	11.0	13.5	2.9	1.2

In order to study the effect of heat treatment on austenite phase fraction and austenite stability, all specimens were austenitized in a vacuum furnace at 885°C for 1 h followed by controlled cooling with a cooling rate of 10°C/ min. Half of the samples were treated cryogenically in a freezing unit at –73°C for 1 h. For TEM investigations the samples were tempered at 600°C for 5 h in a batch furnace.

In-situ XRD measurements were conducted to determine the austenite phase fraction in the as quenched and refrigerated condition as well as during tempering at 540°C and 600°C for 5 h. All XRD investigations were carried out using a Bruker™ AXS Advance diffractometer with an Anton Paar™ (HTK2000) high temperature chamber. Cr-K_α radiation was used with a wavelength of 2.29 Å. For the quantitative determination of phase fractions the Rietveld method [14] was applied. Measuring time for each diffractogram was set to 37 min. Because of the relatively short measuring time, measuring inaccuracy of austenite phase fraction was about ±1-3 wt.%.

TEM measurements were performed with a Philips™ CM12 microscope. Samples of 3 mm in diameter were ground to 80 µm and subsequently electrolytically etched using a Struers™ A2 electrolyte. Chemical composition was studied via an energy dispersive X-ray spectroscopy (EDS) detector attached to the microscope.

Dilatometric measurements were carried out using a TA Instruments™ (formerly BAEHR™) DIL 805A dilatometer. Tempering treatment was performed at 540°C and 600°C for 1 h and 5 h. The samples for the dilatometer analysis were tubular with a length of 10 mm, an outer diameter of 4 mm and a wall thickness of 1 mm. The heating and cooling rate was set to 100°C/ min. Quenching to –100°C was done by a freezing unit from TA instruments™ with the aid of helium, which was cooled before with liquid nitrogen and passed through the hollow dilatometer samples. Discontinuous length changes of the specimen during the thermal cycle were taken as indication for austenite to martensite phase transformation, as this phase transformation is linked with a volumetric change. Measuring inaccuracy of martensite start (Ms) temperature was ~10°C.

2. Results

2.1. *In-situ* measurements of austenite phase fraction during tempering

(Fig. 1) presents the results of phase fraction analyses of austenite during tempering at different temperatures. After quenching from austenitizing temperature retained austenite is present as indicated by the values for tempering time 0 h. The content of retained austenite in this condition is ~6 wt.%. By performing a cryogenic treatment the austenite phase fraction is reduced to approximately 2 wt.%.

Subsequent tempering treatment after austenitization or after cryogenic treatment causes an increase of austenite phase fraction. This increase is related to the formation of reverted
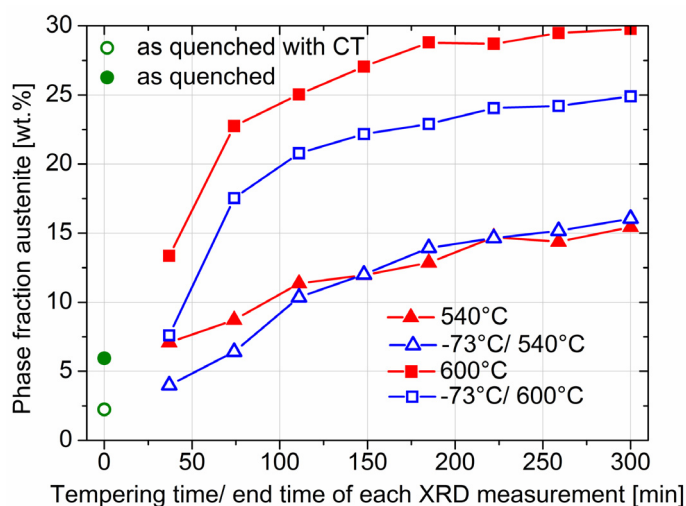
Fig. 1. Analysis of the phase fraction of austenite directly after quenching from austenitization temperature or cryogenic treatment (CT) (circles) and during tempering at 540°C (triangles) and 600°C (squares) for 5 h for CT and non-CT samples. Each measuring point indicates a XRD measurement during tempering or before tempering. The time increment of these graphs correspond to the measurement time for each XRD measurement, i.e. 37 min

austenite. After 5 h of tempering at 600°C the fraction of austenite raises up to ~30 wt.% for the non-CT samples and to ~25 wt.% for the CT samples. Differences in austenite phase fractions at 600°C due to CT may be a result of the measuring inaccuracy. Additionally, it is suggested that CT, which causes a lower phase fraction of retained austenite, may influence the formation process of reverted austenite. After 5 h of tempering at 540°C about 15 wt.% austenite are present for CT as well as for non-CT samples. Consequently, tempering at 600°C causes a much more pronounced formation of reverted austenite than tempering at 540°C.

2.2. Characterization of the microstructure after heat treatment

In (Fig. 2a) the martensitic microstructure after austenitizing is illustrated. Retained austenite films are determined at martensite lath boundaries via selected area diffraction and corresponding dark-field images (Fig. 2b). The average thickness of retained austenite films is approximately 20 nm.
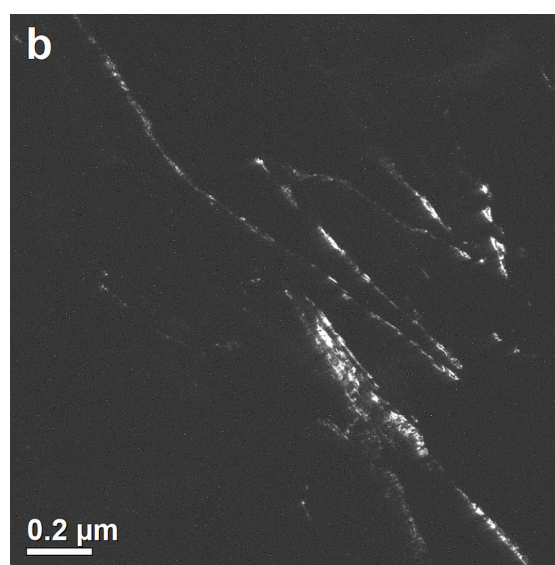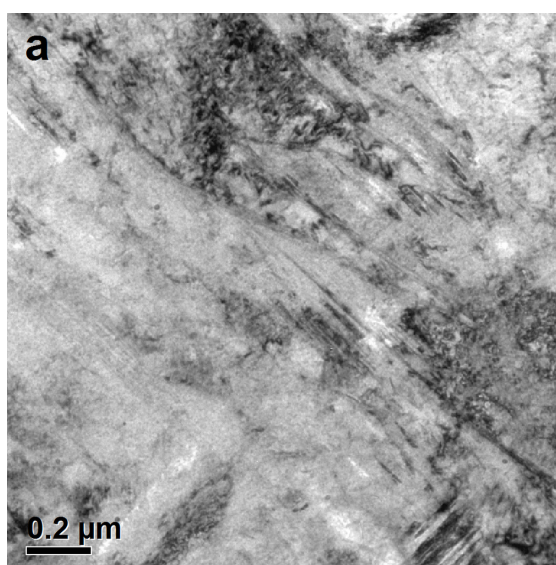

Fig. 2. TEM analysis of martensitic matrix and retained austenite of a sample, which was austenitized at 885°C for 1 h and quenched to room temperature. The bright-field image (a) and the corresponding dark-field image (b) show retained austenite films at martensite lath boundaries

In (Fig. 3) the microstructure of a sample tempered at 600°C for 5 h without CT is depicted. In this case austenite is still present at martensite lath boundaries and austenite films have grown to size of approximately 200 nm in thickness. It should also be noticed that carbide precipitation occurs, as described in [15].

In order to study chemical compositions of austenite and martensite after tempering at 600°C EDS, measurements were employed. The results are summarized in (Table 2). Apparently, the nickel content of the reverted austenite is enhanced in contrast to the nickel content of martensite. In contrast to that, cobalt content in reverted austenite is reduced.

As TEM investigations on CT samples do not show any distinct differences to non-CT samples, analyses are not presented in this paper.

TABLE 2

Measurement of the chemical composition via EDS analyses of austenite and martensite after 885°C/ 1 h/ 600°C/ 5 h

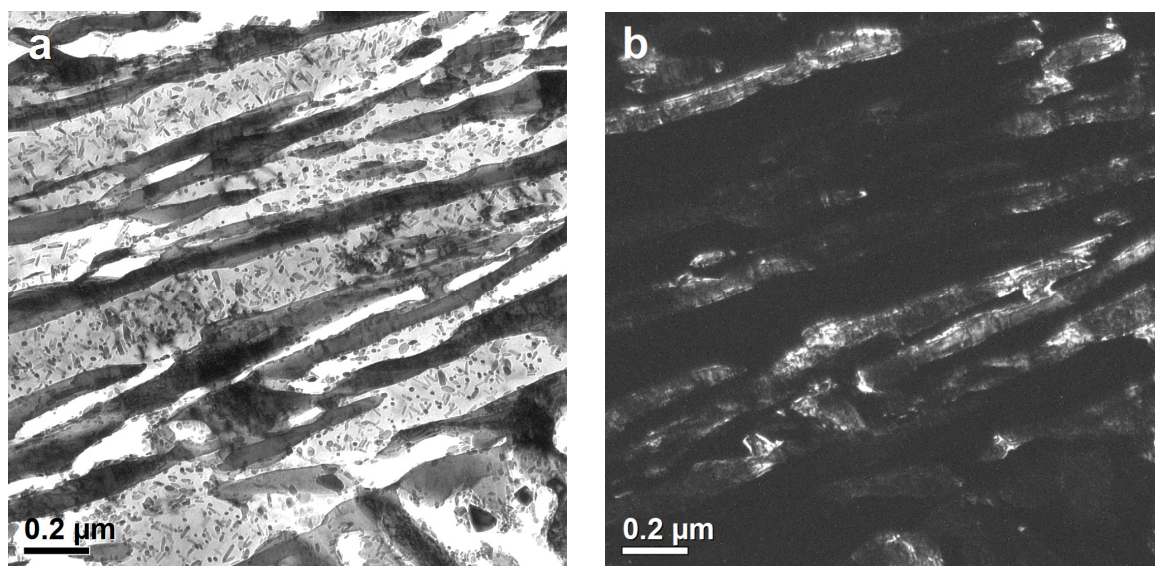|	Ni [wt.%]	Co [wt.%]	Cr [wt.%]	Mo [wt.%]	Fe [wt.%]
Reverted austenite	18.2	11.0	5.6	1.5	63.7
Martensite	9.2	13.3	5.4	1.2	70.8

2134

Fig. 3. TEM images showing tempered martensite, reverted austenite and carbides. Samples were austenitized at 885°C for 1 h, quenched to room temperature and tempered at 600°C for 5 h. The bright field image (a) and the corresponding dark field image (b) show reverted austenite films at martensite lath boundaries

2.3. Characterization of the transformation behavior of austenite

For characterizing the stability of austenite, its transformation behavior during cooling was studied by dilatometric investigations. In (Fig. 4) the relative length change during cooling to −100°C after tempering at 540°C for 1 h and for 5 h with and without CT is illustrated. For the purpose of good comparability of the results, the cooling curves were shifted in the direction of the relative length change axis. Therefore, no scaling is shown for this axis. From these measurements it can be deduced that a volume increase occurs during cooling after tempering at

540°C for 1 h and for 5 h with and without CT. The increase of volume during cooling is related to a phase transformation of austenite to martensite, as the phase transition from austenite to martensite is accompanied by a volume increase. (Fig. 4) shows that transformation of austenite is less intense with increasing holding time and with previous cryogenic treatment.

Additionally, dilatometric investigations were carried out for tempering at 600°C for 1 h and 5 h for CT and non-CT treated samples. Cooling curves after tempering are depicted in (Fig. 5). Again, the relative length change axis is not scaled, because curves were shifted for the purpose of good comparability. During cooling after tempering at 600°C again a martensitic trans-
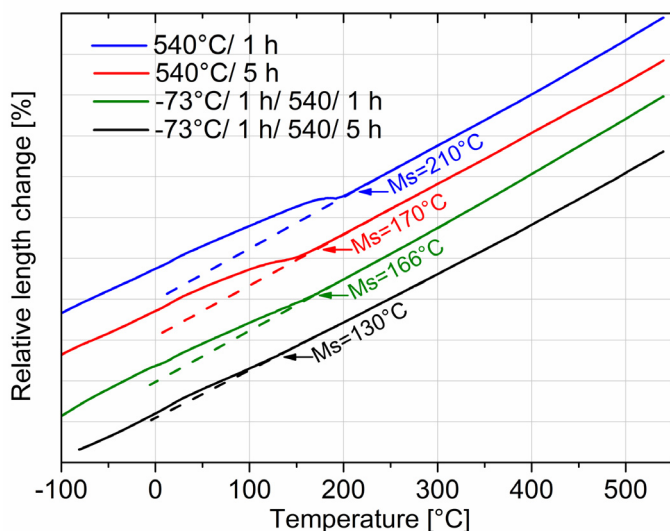

Fig. 4. Dilatometric cooling curves of the CT and non-CT samples after a tempering treatment at 540°C for 1 h and for 5 h. Curves show a martensitic transformation during cooling, which is less intense and starts at lower temperatures with longer holding times and with the application of a previous cryogenic treatment
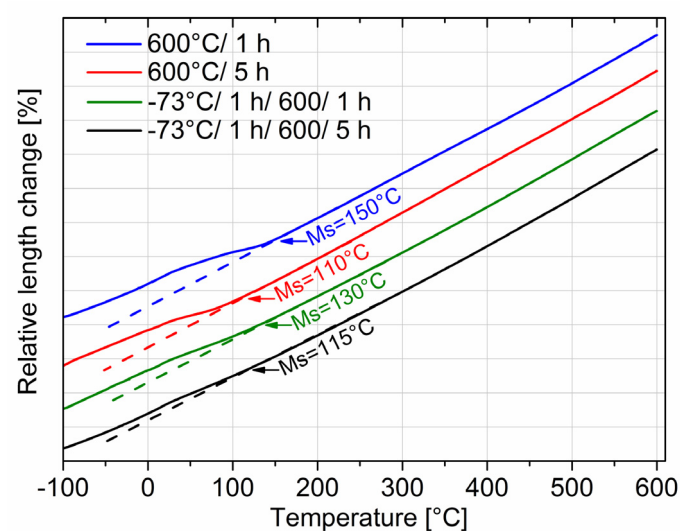

Fig. 5. Dilatometric cooling curves of the CT and non-CT samples after a tempering treatment at 600°C for 1 h and for 5 h. Curves show a martensitic transformation during cooling, which is less intense and starts at lower temperatures with longer holding times and with the application of a previous cryogenic treatment

formation occurs. Also in this case, martensitic transformation of austenite during cooling after tempering at 600°C is weaker for CT samples and for samples which were tempered for 5 h.

The martensite start (Ms) temperature was determined by the first deviation from the linear behavior of relative length change curve during cooling. This was done because the cooling curves behave slightly different when martensitic transformation has started. In (Fig. 4) and (Fig. 5) *Ms* temperatures of all tempering treatments are presented. From the analysis of *Ms* temperatures it can be deduced that *Ms* temperature is lower the higher the tempering temperatures and the longer the tempering times are. Also CT reduces the *Ms* temperatures in most cases, except for tempering at 600°C for 5 h.

3. Discussion

Phase fraction measurements by XRD indicate that the austenite content is 6 wt.% after quenching from austenitizing and 2 wt.% after CT. During subsequent tempering an increase of austenite phase fraction due to formation of reverted austenite was determined by *in-situ* high temperature XRD measurements. After 5 h of tempering the austenite phase fraction is approximately 15 wt.% for the samples tempered at 540°C and 25-30 wt.% for the samples tempered at 600°C.

Microstructural characterization via TEM investigations demonstrated that retained austenite after quenching from 885°C as well as reverted austenite after tempering at 600°C for 5 h is located at martensite lath boundaries. Films of retained austenite exhibit a thickness of about 20 nm, whereas reverted austenite films have grown to a thickness of about 200 nm. From position of occurrence and growth behavior of the austenite films it is suggested that reverted austenite mainly nucleates at retained austenite. Composition of austenitic regions after tempering at 600°C for 5 h shows a clear enrichment of nickel. This is in good correlation with the literature dealing with nickel enrichment in reverted austenite [2,9,16].

Dilatometric investigations of cooling behavior after tempering reveal that martensitic transformation is less intense and occurs at lower temperatures with higher tempering temperatures, longer tempering times and with the application of a cryogenic treatment at –73°C. As the resistance of austenite against its transformation can be correlated with the stability [17], *Ms* temperatures were used to characterize the stability of austenite after different heat treatments. The higher the *Ms* temperature is the lower is the stability of austenite. Therefore, it can be assumed that the austenite stability is higher after longer tempering times, higher tempering temperatures and with the application of a CT. In order to explain these differences due to different tempering treatments, it is necessary to understand the mechanism of austenite stabilization during tempering. Therefore, equilibrium calculations as well as diffusional calculations were carried out with MatCalc [18-20]. As nickel is the element, which stabilizes austenite [5], equilibrium calculations of nickel distribution in austenite and ferrite at 540°C and 600°C were

performed for the composition given in (Table 1). Simulations reveal that nickel concentration is higher in austenite compared to ferrite, as nickel concentration in austenite is predicted to be 31.6 wt.% and 25 wt.% for the equilibrium condition at 540°C and 600°C, respectively. Thus, the stability of austenite should be higher at 540°C which does not agree with the experimental results in this work. As a consequence of this, the varying stability of austenite is probably originated by the kinetics of nickel transport at 540°C and 600°C. Also, Schnitzer et al. [9] described that formation of reverted austenite is controlled by the diffusion of Ni to an austenite nuclei. It is assumed that reverted austenite is enriched with nickel from the beginning of its creation, which is also in good agreement with the higher Ni concentration in equilibrium austenite at 540°C and 600°C. According to these findings, it can be followed that reverted austenite is more stable from the beginning of formation due to enrichment of nickel than the retained austenite. However, from a thermodynamic point of view it is suggested that retained austenite also gets enriched in nickel during tempering by diffusion of nickel from the adjacent reverted austenite into the retained austenite. As this stabilization effect is diffusion controlled, *Ms* temperatures versus the diffusion lengths of nickel as defined in Eq. (1) are depicted in (Fig. 6).

Diffusion coefficients of nickel in austenite were calculated at 540°C and 600°C by using MatCalc and the composition in (Table 1). The diffusion lengths x of the various tempering times t were derived from the diffusion coefficients D and the Eq. (1) for the mean diffusion path [21,22].

$$x = \sqrt{4Dt} \qquad (1)$$

In (Fig. 6) it is shown that the diffusion length of nickel in austenite increases with higher tempering temperatures and longer tempering times. It is also derived that *Ms* temperature of non-CT as well as of CT samples decreases with increasing diffusion length of nickel in austenite. Consequently, it is argued that stabilization of austenite is controlled by diffusion of nickel in austenite. On the one hand diffusion of nickel into retained austenite leads to stabilization due to nickel enrichment, on the other hand the size of non-stabilized austenite is reduced which also may lead to stabilization. Therefore, it can be summarized that the higher the tempering temperatures and the longer the tempering times are, the higher the stabilization of austenite due to nickel diffusion into austenite is.

Furthermore, the findings from (Fig. 6) can be described with the relationship found in literature [6,23,24], which assumes that the probability of finding a defect that can act as a nucleus for the martensitic transformation is proportional to the volume of the non-stable austenite film. The probability of finding such a defect can be related to the *Ms* temperature because the more nucleation sites are present the higher the probability for martensitic transformation is. A higher probability for martensitic transformation leads to a higher martensite start temperature. The size of the non-stabilized austenite can be correlated with the diffusion length of nickel in austenite.

2136

The longer the diffusion length of nickel in austenite is, the more the retained austenite gets stabilized. It is suggested that stabilized austenite does not participate in martensitic transformation. Hence, thickness of non-stabilized austenite is getting smaller due to stabilization because of Ni diffusion into austenite which results in a lower effective thickness of unstable retained austenite films and a lower probability of finding a defect for martensitic transformation. This leads to a lower *Ms* temperature for thinner unstable austenite films, which is in agreement with the findings in this work.

It is also shown in (Fig. 6) that *Ms* temperature is lower for the CT samples. As the main difference between CT and non-CT samples is the content of retained austenite, it is argued that the less intense martensitic transformations of the CT samples are due to the lower content of non-stabilized retained austenite. Additionally, it is supposed that the average size (mainly the thickness) of retained austenite is smaller due to CT treatment and therefore austenite grains exhibit a higher stability, which may lead to the decrease of martensite start temperature due to CT treatment. It should be noticed that the decrease of *Ms* temperature and the less intense transformations due to cryogenic treatment also supports the assumption that mainly retained austenite is not stable after tempering and needs to be stabilized with nickel during tempering. Additionally, by further comparing the behavior of CT and non-CT samples in (Fig. 6) it is asserted that the slope of the curve for CT samples is smaller compared to the curve for the non-CT samples. Hence, it can be followed that this is also due to the reduced average thickness of retained austenite after cryogenic treatment. Because retained austenite is smaller, stabilization due to tempering is not that pronounced compared to non-CT samples.

4. Conclusions

From *in-situ* XRD measurements, dilatometry analyses and TEM investigations the influence of combined heat and cryogenic treatments on the stability of austenite was evaluated and leads to the following conclusions:

- After quenching from austenitizing treatment 6 wt.% austenite remains untransformed. This retained austenite is preferentially located at martensite lath boundaries in form of thin films. Due to subsequent cryogenic treatment austenite phase fraction is reduced to 2 wt.%.
- During tempering at 600°C and 540°C reverted austenite is formed. As reverted austenite is also located at lath boundaries, it is suggested that reverted austenite mainly nucleates at retained austenite.
- From dilatometer investigations it is derived that austenite is more stable after tempering, when tempering was performed at higher temperatures and longer times. Also cryogenic treatment before tempering seems to enhance stability of austenite.
- It is demonstrated by comparing the transformation behavior of CT and non-CT samples that mainly retained austenite transforms during cooling. Retained austenite is stabilized as a result of tempering due to nickel diffusion in austenite from reverted into retained austenite.
- Furthermore, it can be concluded that retained austenite can be stabilized via tempering treatment and stabilization is dependent on the diffusion length of nickel at different temperatures.

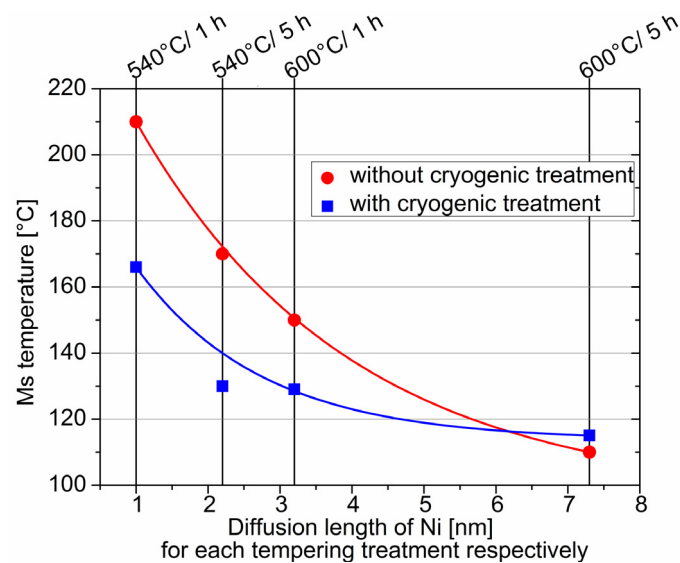Fig. 6. Martensite start (Ms) temperature as a function of the diffusion length of Ni in austenite for each heat treatment

REFERENCES

[1] P.M. Novotny G. E. Maurer, Adv. Mater. Process, 37-40 (2007).
[2] R. Ayer, P.M. Machmeier, Metall. Trans. A **24A**, 1943-1955 (1993).
[3] K. Sato. Improving the Toughness of Ultrahigh Strength Steel. PhD thesis, University of California (2002).
[4] M. Gruber. Mikrostruktur und mechanische Eigenschaften der Aermet 100 Legierung. Diploma thesis, University of Leoben (2012).
[5] G. Haidemenopoulos. Dispersed-Phase Transforamtion Toughening in Ultrahigh-Strength Steels. PhD thesis, Massachusetts Institute of Technology (1988).
[6] G. Haidemenopoulos, M. Grujicic, G. Olson, M. Cohen, J. Alloy. Compd. **220**, 142-147 (1995).
[7] J. Wang S. v. d. Zwaag, Metall. Trans. A **32A**, 1527-1539 (2001).
[8] T. Waitz, T. Antretter, F. Fischer H. Karnthaler, Mater. Sci. Technol. **24**, 934-940 (2008).
[9] R. Schnitzer, R. Radis, M. Nöhrer, M. Schober, R. Hochfellner, S. Zinner, E. Povoden-Karadeniz, E. Kozeschnik H. Leitner, Mater. Chem. Phys. **122**, 138-145 (2010).
[10] H.K.D.H. Bhadeshia, D.V. Edmonds, Met. Sci. **17**, 411-419 (1983).

[11] R. Ayer, P. M. Machmeier, Metall. Trans. A **27A**, 2510-2517 (1996).

[12] H.E. Lippard. Microanalytical Investigations of Transformation Toughened Co-Ni Steels. PhD thesis, Northwestern Universitiy, Evanston Illinois (1999).

[13] C.J. Kuehmann. Thermal processing optimation of nickel-cobalt ultrahigh-strength steels. PhD thesis, Northwestern University, Evanston, Illinois (1994).

[14] R.A. Young, The Rietveld Method, Oxford Universitiy Press, New York 2002.

[15] M. Gruber, S. Ploberger, M. Wiessner, S. Marsoner, R. Ebner, Work presented at the International Conference on Martensitic Transformations 2014, Bilbao Spain.

[16] M. Farooque, H. Ayub, A. UlHaq and A. Kahn, J. Mater. Sci. **33**, 2927-2930 (1998).

[17] A. Kokosza, J. Pacyna, Arch. Metall. Mater. **55**, 1001-1006 (2010).

[18] E. Kozeschnik, MatCalc Version 5.61, Vienna University of Technology.

[19] MatCalc, Thermodynamic Database "mc_fe_V2.040", Vienna University of Technology.

[20] MatCalc, Mobility Database "mc_fe_V2.006", Vienna University of Technology.

[21] A. Einstein, Ann. Phys. 549-560 (1905).

[22] H.K.D.H. Bhadeshia, http://www.msm.cam.ac.uk/phase-trans/mphil/MP6-3.pdf.

[23] R. Cech, D. Turnbull, Trans. AIME, 124-132 (1956).

[24] M. Cohen, G. Olson, New aspects of Martensitic Transformation, First Japan Institut of Metals, 93-98 (1976).